EARTHQUAKE SPECTRA

The Professional Journal of the Earthquake Engineering Research Institute

Bayesian estimation of macroseismic intensity from post-earthquake rapid damage mapping

M. Pittore [a], L. Graziani [b], A. Maramai [b], M. Haas [a], S. Parolai [c] and A. Tertulliani [b]

The seismological community acknowledges the essential contribution of macroseismic assessment to the compilation of the seismic catalogues used for seismic hazard assessment. Furthermore, macroseismic observations are routinely employed by Civil Protection authorities in the aftermath of damaging events to improve their decision making capacity. In this contribution, we describe a novel methodology for the rapid, probabilistic estimation of the Macroseismic Intensity in the epicentral area of a major event, according to the European Macroseismic scale (EMS-98). The methodology includes the use of mobile mapping and a collaborative on-line platform for rapid post-earthquake reconnaissance, A Bayesian scheme is proposed to integrate direct damage observations and prior information, hence allowing the consideration of ancillary data and expert judgment. According to a feasibility study that has been carried out in the area affected by the 2016 Amatrice (Central Italy) earthquake, the proposed methodology may provide a reliable estimation of intensity, efficiently integrating further post-earthquake building damage surveys.

INTRODUCTION

Macroseismic Intensity (hereinafter MI) is a measure of the overall ground shaking that an area has been exposed to, and is based on the observation of the effects of the ground motion on built structures, the environment and the population's reaction. Many different scales have been proposed for this scope, in different regions (see, e.g., Musson, 2012) over the last decades. A widely used scale is the Modified Mercalli Intensity (MMI) (Wood and Neumann, 1931), originally derived in 1931 from the earlier version of the Mercalli-Cancani-Sieberg (MCS) (Sieberg, 1931) scale. A more recent evolution of the MMI scale is still used in USA by USGS (Stover and Coffman, 1993; Bormann, 2011) while in Italy the Dept. of Civil Protection routinely employs the MCS scale (Galli et al., 2016). In 1965, based on available MCS observations,

[a] Helmholtzcentre Potsdam German Research Centre for Geosciences, Potsdam, Germany
[b] Istituto Nazionale di Geofisica e Vulcanologia (INGV), Rome, Italy
[c] Istituto Nazionale di Oceanografia e di Geofisica Sperimentale (OGS), Trieste, Italy

the MSK-64 scale was proposed (Richter, 1958; Medvedev et al., 1965). This scale has been widely used in Europe, Russia and Central Asia, while in China and Japan, different MI scales are used that have not been derived from the original Mercalli one (Musson et al., 2010). More recently, an international committee proposed a revised and extended version of the MSK-64 scale (and the subsequent MSK-81 version), termed EMS-98 (Grünthal, 1998). Early intensity scales generally dealt with damage in a limited way, for instance stating that for a certain intensity, a certain damage scenario would occur. However, apart from some generic descriptions of building types (good designed, well built, poorly built etc.), no vulnerability classifications were used. The MSK scale first introduced both a qualitative and quantitative approach to damage, which has been further developed in the formulation of the EMS-98 scale, supported by a more differentiated set of building types associated with a level of physical vulnerability (Musson et al., 2010).

The EMS-98 scale was intended to be used throughout Europe, although it was derived using also data from other regions as well. It was also meant to contribute to bridging the gap between seismologists and engineers, especially after the recent development of new types of buildings, including earthquake resistant design structures, not considered previously. In the last decade interest in MI has grown and the seismological community acknowledges its essential contribution to seismic hazard assessment. In particular, in Italy, MI is the basis of the compilation of the seismic catalogues, and is still the only tool for providing a confident comparison with historical earthquakes and their impact on the territory. For this reason macroseismic techniques should be continuously reviewed and improved in order to obtain the highest level of accuracy. Currently in Italy, two types of macroseismic assessments are employed in the aftermath of a damaging earthquake. First, an initial survey is carried out in collaboration with the Department of Civil Protection using the MCS intensity scale in order to provide a preliminary mapping of the damage distribution and improve the management of the emergency phase. The use of the MCS scale for the first survey has been motivated so far by its simpler implementation schema, leading to a prompter estimation of the extent of damage. However this scale does not allow a proper consideration of the type and vulnerability of the buildings, but only provides the overall damage description. Next, a more refined assessment is performed with the aim of defining the damage scenario in terms of EMS-98 (Azzaro et al., 2016). To this purpose, the emergency group of INGV (Istituto Nazionale di Geofisica e Vulcanologia), referred to as QUEST (Quick Earthquake Survey Team), is activated to undertake the macroseismic field survey. On 24 August 2016, soon after the Mw 6.0 shock that occurred in the

Rieti province (Central Italy), the first of a long and disastrous sequence of events that claimed the lives of about 300 people in the Amatrice area (Anzidei and Pondrelli, 2016), several teams of QUEST started their surveys, visiting the localities within the epicentral area. From August 24 to the end of September 2016, a thorough macroseismic intensity assessment for 140 target locations in the epicentral area was carried out, considering the different building typologies, their vulnerability, and the damage they suffered, and assessing the EMS-98 intensity (Azzaro et al., 2016). This involved a total of about 20 expert surveyors, split into small groups of 2-3 people, walking across the most affected areas and noting the consequences that were visible on the exterior of the buildings. Although this approach allows a precise mapping of the damage, it also has several potential drawbacks: it is resource- and time-intensive, it entails field activities that may be adversely affected by the environmental conditions, and the surveyors often have to visit heavily damaged areas, therefore being exposed to further collapses or falling debris, especially in case of strong aftershocks.

In order to overcome these limitations, a novel methodology to estimate the MI across an epicentral area, according to the EMS-98 scale, is described in this paper. The methodology allows one to rapidly and safely collect building-by-building data on the observed damage in the hours and days immediately following a destructive event, and to provide a probabilistic estimation of MI at the settlement aggregation level. The methodology employs an innovative platform to map damage to built structures using geo-referenced omnidirectional images, and a Bayesian updating scheme able to accommodate different types of observations and prior information, hence allowing a flexible case-by-case customization. A feasibility study has been carried out in the area affected by the above mentioned 2016 Amatrice (Central Italy) earthquake and validated with the data provided by INGV. The obtained results are encouraging and show that the proposed technique may contribute to a prompt, sound and automatic preliminary assessment of EMS-98 intensity which could efficiently integrate the current operational protocols.

In the next section the proposed methodology will be introduced and the employed datasets described. This is followed by a section covering the results obtained in Italy. A discussion section is then provided, followed by the conclusions and outlook.

METHODOLOGY

DATA COLLECTION AND ANALYSIS

A customized mobile mapping system, originally designed for seismic exposure and vulnerability characterization (Pittore and Wieland, 2013; Pittore et al., 2015) has been employed to rapidly collect geo-referenced omni-directional images of the built environment. The system is composed of an omnidirectional camera with 5 synchronized optical units, a low-cost GNSS system and a data collection and processing unit. The camera can be easily and promptly fixed to the roof of a vehicle by means of four sucking cups, and records geo-referenced high-resolution (2 MPixels per optical unit) images at rates between 5 and 15 frames per second. Once mounted and switched on, the system is driven across the area to be investigated. In a post-processing phase, the cameras' streams are stitched together into a sequence of omnidirectional images, in equirectangular projection. These images are then further filtered based on their mutual distance, in order to have a uniform spatial coverage along the driven path. Since a complete coverage of the affected areas would be time-consuming and in most case just unfeasible due the constraints of the emergency management, the images are collected following a statistical sampling approach (Pittore et al., 2015). A stratification scheme has been followed to ensure a balanced coverage of the damage distribution in the field. In this case study presented the damage grading made available by the Copernicus Emergency Service [a] has been used as a basis for the stratification. Lacking such information different approaches could be followed to estimate a suitable proxy upon which to perform the sampling, e.g., using a combination of prior information on the vulnerability and on the expected intensity.

Routing optimization: the Copernicus Emergency Mapping service

The Copernicus Rapid Mapping service provides rapid grading of damage and serviceability of buildings and roads in the areas most affected by natural events such as floods, earthquakes or tornadoes (Boccardo and Tonolo, 2015; Freire et al., 2015). Different GIS layers, in the form of print-ready maps and digital data (ESRI shapefiles) are produced as soon as remote sensing data is available. In the case of the 24 August Amatrice earthquake, the information was provided by the Emergency Mapping Service in less than three days after the occurrence of the earthquake, consisting of a damage grading of 5'875 buildings in the epicentral region (Copernicus, 2016). The grading is based on the manual comparison of pre-event 0.5m and 0.2m orthophoto data (

[a] http://emergency.copernicus.eu/

2014 CONSORZIO TeA) with aerial (acquired August 25th 2016 10:00 UTC, GSD 0.1 m, 0% cloud coverage) and satellite images (acquired on August 25th 2016, 9:45 UTC, WorldView-2, GSD 0.5 m, approx 15% cloud coverage, 34 and 31 off-nadir angles). The grading was made available on 27 August, and covers an area of approximately 500 km^2, as shown in Fig. 1.

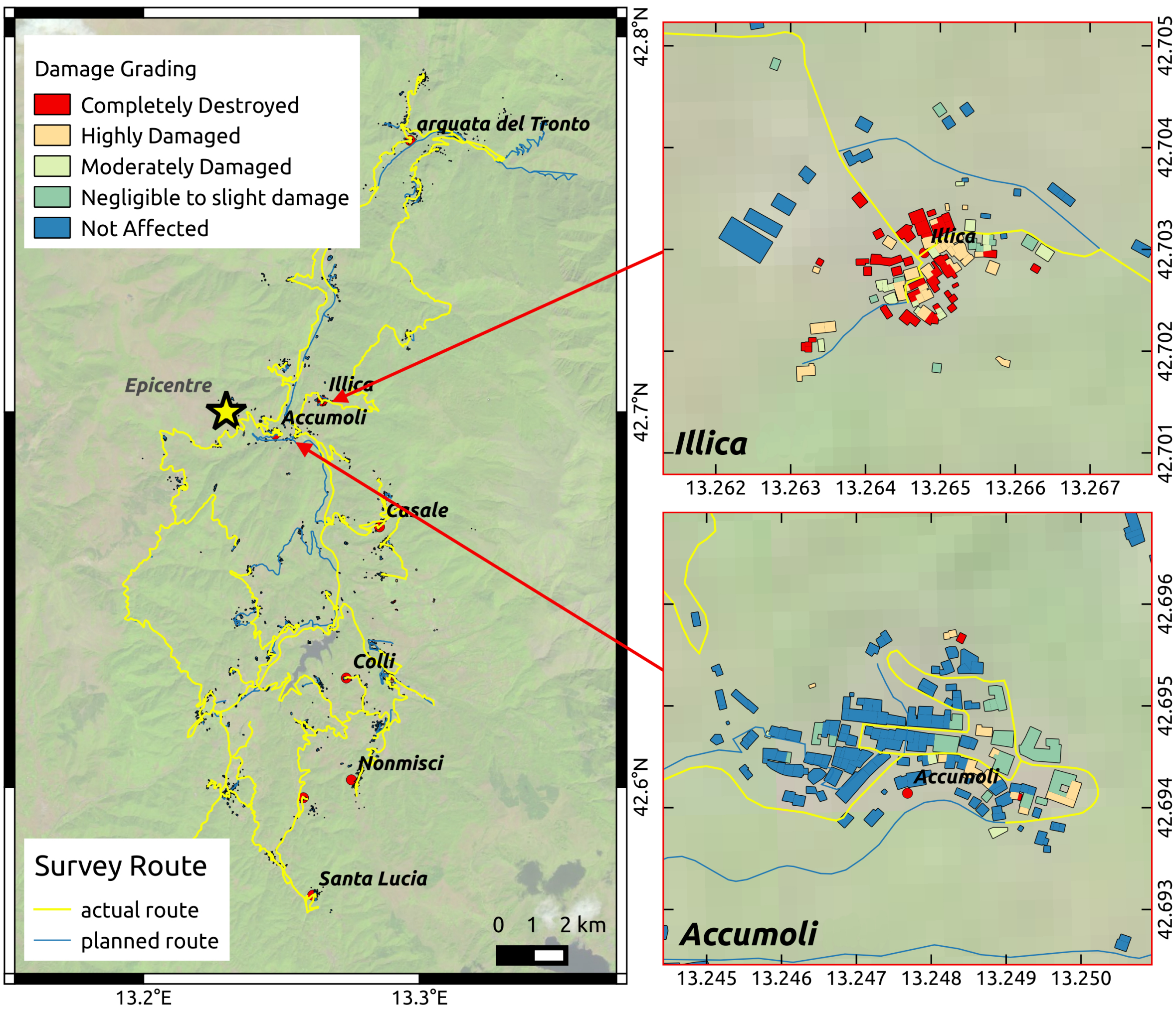

Figure 1. Overview of the study area subjected to grading from the Copernicus Rapid Mapping service. The inset shows a close-up of the building-by-building grading in the towns of Accumoli and Illica (in the Rieti provincial district).

The mapped buildings have been assigned a damage grade ranging from *not affected* to *completely destroyed*, with the intermediate cases: *negligible to slight damage*, *moderately damaged* and *highly damaged*. Although this damage scale is expectedly different from the one proposed by EMS-98, it still conveys useful information on the general damage pattern in the area. The sampling has been performed in two stages:

- first by sampling a percentage (5%) of buildings in each of the 5 damage grades and automatically computing an optimal route path linking them over the road network extracted from OpenStreetMap, and

- randomly selecting a set of buildings from the available footprints lying within a 30m buffer from the route actually followed by the mobile mapping system.

The planned route is also shown in Fig. 1, along with the route actually followed. The route was covered in around two days between September 26th and 28th 2016, and more than 50'000 omnidirectional images were collected. A subset of 9'900 images were then selected based on a minimal distance of 5 meters between each image.

Rapid Remote Damage Assessment (RRDA)

In order to carry out a rapid, remote mapping of the physical damage to buildings, a dedicated web-based on line platform has been developed (see Fig. 2). Making use of this interface, a pool of three expert surveyors from INGV analyzed the captured omni-directional images and provided an assessment of the observable damage according to the grades defined by the EMS-98 scale (listed in Table 1), as well as the most probable EMS-98 vulnerability class (decreasing from class A to class F, being class A the most vulnerable, and class F the most resistant), for a set of specific buildings.

Table 1. Damage grades proposed by the EMS-98 scale for masonry and reinforced concrete buildings.

Damage	Description	
	Masonry	Reinforced Concrete
D1 (Slight)	Hair-line cracks in very few walls; fall of small pieces of plaster only; fall of loose stones from upper parts of buildings in very few cases.	Fine cracks in plaster over frame members or in walls at the base; fine cracks in partitions and infills.
D2 (Moderate)	Cracks in many walls; fall of fairly large pieces of plaster; partial collapse of chimneys.	Cracks in columns and beams of frames and in structural walls; cracks in partition and infill walls; fall of brittle cladding and plaster; falling mortar from the joints of wall panels.
D3 (Heavy)	Large and extensive cracks in most walls; roof tiles detach; chimneys fracture at the roof line; failure of individual non-structural elements (partitions, gable walls).	Cracks in columns and beam column joints of frames at the base and at joints of coupled walls; spalling of concrete cover, buckling of reinforced rods; large cracks in partition and infill walls; failure of individual infill panels.
D4 (Very Heavy)	Serious failure of walls; partial structural failure of roofs and floors.	Large cracks in structural elements with compression failure of concrete and fracture of rebars; bond failure of beam reinforced bars; tilting of columns; collapse of a few columns or of a single upper floor.
D5 (Destruction)	Total or near total collapse.	Collapse of ground floor or parts (e. g. wings) of buildings.

The platform automatically generates so called *tasks*, each including a set of 100 buildings randomly chosen from the ones previously selected. Each surveyor is assigned one or more of these tasks (the tasks are not overlapping) and as soon as the analysis of one building is completed, the information is uploaded into a centralized database for subsequent processing. The building footprints provided from the Copernicus Emergency Service have been used as a basic geometry. The web interface shows on the right side the selected buildings and the location of the closest omnidirectional images (Fig. 2,A). The selected image is shown on the left side of the interface, and can be zoomed or paned. The lower side of the interface contains the list of buildings in the task with their status (*Unmodified*, *Modified*, *Completed*), a set of drop-down menus to specify the damage and vulnerability and a free text area for additional comments. Fig. 2 shows for instance a building which has been assigned EMS-98 vulnerability A and damage grade 3. The RRDA interface also allows to query for the closest omni-directional image available from the Google StreetView service. This allows a direct comparison of the appearance of the building before and after the earthquake (Fig. 2, B-C). This is useful for better characterizing the vulnerability of the building and also to ascertain whether pre-event damage was already present.

For this preliminary analysis a total of 500 buildings from around 20 different settlements were analyzed. In order to decrease the chances of possible bias, the surveyors were given no information about the name of the locality, nor the grading assigned by the Copernicus Emergency Service. A total of 313 buildings had damage and vulnerability assigned to them, while for 187 buildings no reliable assignment was given for one or more of the following reasons: the building was partially or totally obstructed by other buildings, walls, fences or vegetation; the building was too far from the camera (hence poor resolution of the image); the image was unsuitable for analysis because it was too dark or too bright.

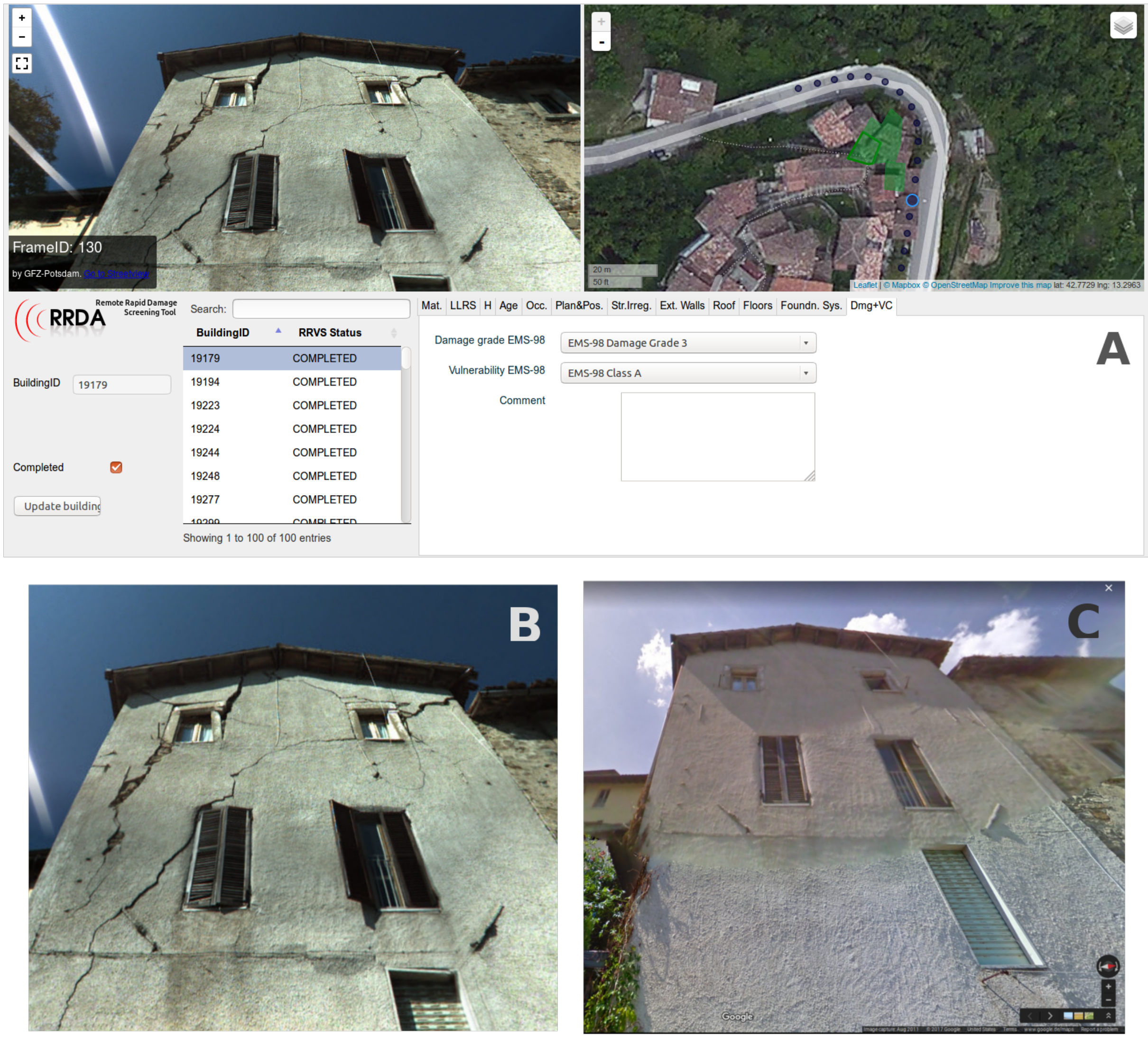

Figure 2. An example of a building selected for inspection and remotely analysed by surveyors. A) The RRDA web-based interface showing on the right side an aerial map with the selected building (green texture) superimposed and the location of the closest omni-directional images (blue dots). On the left the selected omni-directional image can be zoomed and panned (or visualized full-screen). The lower part of the interface lists the buildings of the task (each building can be selected by clicking on the corresponding item in the list) and the drop-down menus for entering the observed damage and vulnerability class. B) Omni-directional image captured by the mobile mapping system. C) Corresponding pre-event omnidirectional image from the Google StreetView$^{\text{TM}}$service.

The individual building observations have been spatially aggregated over the set of target locations where MI assessment had already been carried out by INGV. Due to the lack of specific administrative boundaries, in order to assign a geographical location to each of the individual grading a Voronoi tessellation (Watson, 1993) has been generated from the coordinates of the localities with assigned MI, and each graded building has been assigned a locality's name according to the Voronoi cell containing it (see Fig. 3). The same Voronoi tessellation has been employed to aggregate the buildings graded by the Copernicus Emergency Service.

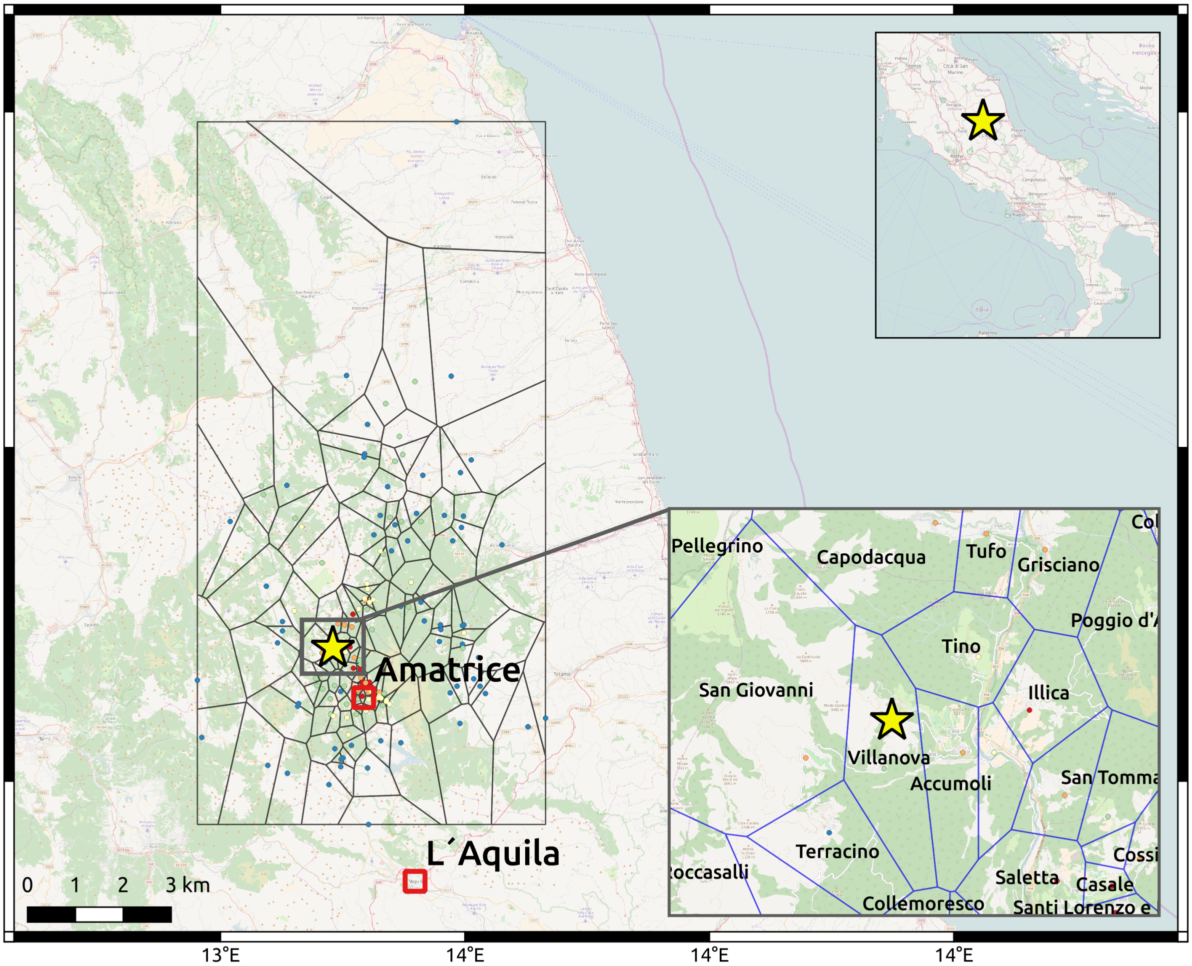

Figure 3. Overview of the considered region with the Voronoi tessellation based on the coordinates of the considered localities. The star marks the location of the epicenter.

BAYESIAN ESTIMATION OF MACROSEISMIC INTENSITY

Since the estimation is carried out in a probabilistic framework the MI in the following is represented by a discrete probability distribution, defined over the range of values $I, II, \cdots, XII$[a], and refers to specific spatial regions (usually corresponding to settlements of different size and geographical extent), referred to as localities. For each of the considered localities the MI (in EMS-98) originally assigned by the pool of experts from INGV is also available (referred to as

[a]The values of macroseismic intensity are usually described by roman numerals, in order to highlight their ordinal nature. For the sake of simplicity throughout the text we will also use an integer notation, without this implying any further assumption

assigned).

The proposed procedure is based on a multi-stage Bayesian updating (see, e.g., Gelman et al., 2004). At each stage the expected discrete probability distribution for the MI is evaluated, using the Bayes rule to integrate different types of available information. A suitable posterior distribution of MI represents the output of each stage, and is used in turn as prior in the subsequent stage:

$$p(I = \hat{I}|D) = \frac{p(D|I = \hat{I})p(\hat{I})}{p(D)} \tag{1}$$

where $p(I = \hat{I}|D)$ indicates the posterior probability of a given intensity $\hat{I}$ conditional on the observed damage scenario D, $p(\hat{I})$ is the probability of the given intensity $\hat{I}$ prior to the observation (hereinafter referred to as the prior) and $p(D|I = \hat{I})$ represents the likelihood of the intensity $\hat{I}$, defined by the probability of observing the damage scenario D under the hypothesis of the particular intensity $\hat{I}$. The term $p(D)$ is the marginal probability of the damage scenario D, and acts as a normalization function. For each possible value of the MI I, the Bayes rule updates its (posterior) probability as soon as new observations become available, as far as these observations can be correlated with the macroseismic intensity by a proper likelihood function.

The procedure starts with the estimation of an initial prior distribution for the intensity, which can be defined for each individual target location, or for the entire area. Different approaches can be followed for defining a prior distribution, according to the extent and quality of information available in the area:

- uninformative prior. This prior represents the absence of hypothesis on the intensity distribution (e.g., all intensity values are equally probable).
- informative prior. A non-uniform distribution (e.g., some intensity values are expected to be more likely than others) can be defined by considering available information, including the use of forward modeling (e.g. based on an Intensity Prediction Equation) or expert judgment.

In the updating mechanism the prior distribution is increasingly superseded by the evidence collected. However, when the number of observations is small with respect to the investigated population, the choice of the prior may significantly affect the resulting posterior distribution. The likelihood function $p(D|I = \hat{I})$ may take different forms depending on the type of available observations, but should always describe the relationships between intensity and observed damage. Following the EMS-98 scale, given a specific intensity, the expected damage distribution is

Table 2. Definition of EMS-98 macroseismic intensity degrees based on a descriptive statistics of observable damage to buildings of different structural vulnerability (Decreasing from A to F). Only the intensity degrees associated to observable damage are reported. Damage severity is expressed in grades from D1, very slight, to D5 total collapse.

Vuln \ MI	**V** (5)	**VI** (6)	**VII** (7)	**VIII** (8)	**IX** (9)	**X** (10)	**XI** (11)	**XII** (12)
A	Few D1	Many D1 Few D2	Many D3 Few D4	Many D4 Few D5	Many D5	Most D5		
B	Few D1	Many D1 Few D2	Many D2 Few D3	Many D3 Few D4	Many D4 Few D5	Many D5	Most D5	
C		Few D1	Few D2	Many D2 Few D3	Many D3 Few D4	Many D4 Few D5	Most D4 Many D5	
D			Few D1	Few D2	Many D2 Few D3	Many D3 Few D4	Many D4 Few D5	Most D5
E					Few D2	Many D2 Few D3	Many D3 Few D4	Most D5
F						Few D2	Many D2 Few D3	Most D5

qualitatively represented by a description of the expected observable effects on the population and the built and natural environments. In this work we focus in particular on the built environment, where the consequence of the ground shaking can be more objectively observed, even if doing so we are discarding most of information generally used to assess the lowest intensity degrees (less than V). The original formulation of EMS-98 does not provide a precise quantitative assessment of the damage to be expected, but rather a description of the statistical properties of the observed damage across the different classes of vulnerability of the exposed buildings, as shown in Table 2 (Grünthal, 1998).

Table 2 describes the link between the observed damage of buildings of similar structural vulnerability and the corresponding assigned macroseismic intensity. The statistics of damage is qualitatively described by expressions which may only broadly be attributed to precise quantities (e.g., many refer to a range of proportions roughly between 20% and 50%, while most indicate generically a proportion greater than 60%). Although this formulation captures the underlying uncertain nature of such assessments, it is not suited for more quantitative applications. In order to frame this into a mathematically sound framework, we use the formulation proposed by Giovinazzi and Lagomarsino (Giovinazzi and Lagomarsino, 2002), which employs concepts and tools from fuzzy set theory in order to translate the information in Table 2 into a set of Damage Probability Matrices (DPM), preserving as much as possible the underlying probabilistic formulation of uncertainty. For the sake of simplicity, we define the damage scenario D in terms of the aggregated physical damage, described by the expected mean damage grade μ_D:

$$\mu_D = \sum_k k\, p(D = k|\hat{I}) \quad k = 1, \cdots, 5 \tag{2}$$

The mean damage grade depends on the probability of a set of buildings to be in one of the 5 EMS-98 damage grades listed in Table 1 when exposed to a macroseismic intensity $\hat{I}$, and takes values in the interval $[0, 5]$, where the extremes represent respectively the total absence of damage and the complete destruction of the structures. The probability $p(D|\hat{I})$ can be approximated by the observed proportion of buildings in the different damage grades.

We can therefore compute the observed mean damage grades for a settlement (or a significant portion of it), and use them as observed data D in the formulation of the likelihood function, which then takes the following form:

$$p(D|I = \hat{I}) = p(\mu_D|I = \hat{I}) = \sum_{v=A,\cdots,F} p(\mu_D^v|I = \hat{I}, v)\, p(v) \tag{3}$$

where $p(v)$ is the probability of the considered building(s) belonging to EMS-98 vulnerability class v, and is estimated as the proportion of buildings of this vulnerability class in the considered locality, while $p(\mu_D^v|I = \hat{I}, v)$ is the estimated probability of observing a damage pattern equivalent to a specific mean damage grade μ_D^v for buildings of a given vulnerability v subject to the considered intensity value $\hat{I}$ (the theorem of total probability has been used to make explicit the conditional dependence on the vulnerability).

Note: Currently there is no consideration of the uncertainty related to the statistical significance of the mean damage grade when computed with few observations. The updating process should therefore be carried out for a given locality only when enough data would be available. Further statistical analysis is required to include this additional uncertainty in the likelihood function.

The Bayesian updating scheme introduced in Eq. 1 can therefore be formulated as:

$$p(I = \hat{I}|D) = \frac{p(\mu_D|I = \hat{I})p(\hat{I})}{p(\mu_D)} = \frac{\sum_v p(\mu_D^v|I = \hat{I}, v)\, p(\hat{I})\, p(v)}{\sum_v \sum_I p(\mu_D^v|I)\, p(I)\, p(v)} \tag{4}$$

where $p(\hat{I})$ is the prior probability of the considered intensity value. In order to compute the term $p(\mu_D^v|I = \hat{I}, v)$ we employ the simple analytical expression proposed by Giovinazzi and

Lagomarsino (2004) and Lagomarsino and Giovinazzi (2006) to estimate the expected μ_D^v:

$$\mu_D(v_{ind}, \hat{I}) = 2.5 \left[1 + tanh \left(\frac{\hat{I} + 6.25\, v_{ind} - 13.1}{2.3} \right) \right] \qquad (5)$$

where $v_{ind}(v)$ refers to a scalar vulnerability index representing the structural fragility of the buildings, and is related to the EMS-98 vulnerability class $v \in \{A, \ldots, F\}$ by a set of fuzzy membership functions. The likelihood term can be estimated by observing that a building associated with a given EMS-98 vulnerability class (e.g., A) can be related to a probabilistic distribution of the vulnerability index v_{ind} used in Eq. 5. In this work, instead of the fuzzy formulation proposed by Lagomarsino and Giovinazzi (2006), a set of triangular probability distributions has been used to represent v_{ind} as a random variable, as shown in Fig. 4. Analogously, the mean damage grade can be represented as random variable whose conditional distribution is estimated by evaluating Eq. 5 with respect to a sample of values from the distribution of v_{ind}. The probability $p(\mu_D^v | I = \hat{I}, v)$ can therefore be estimated by integrating the obtained probability density function for μ_D over a suitable interval around the observed value, conventionally set to $\mu_D \pm 0.5$ if $\mu_D < 0.5$ or $\mu_D > 4.5$, then the extremes of the interval $[0, 5]$ have been used).

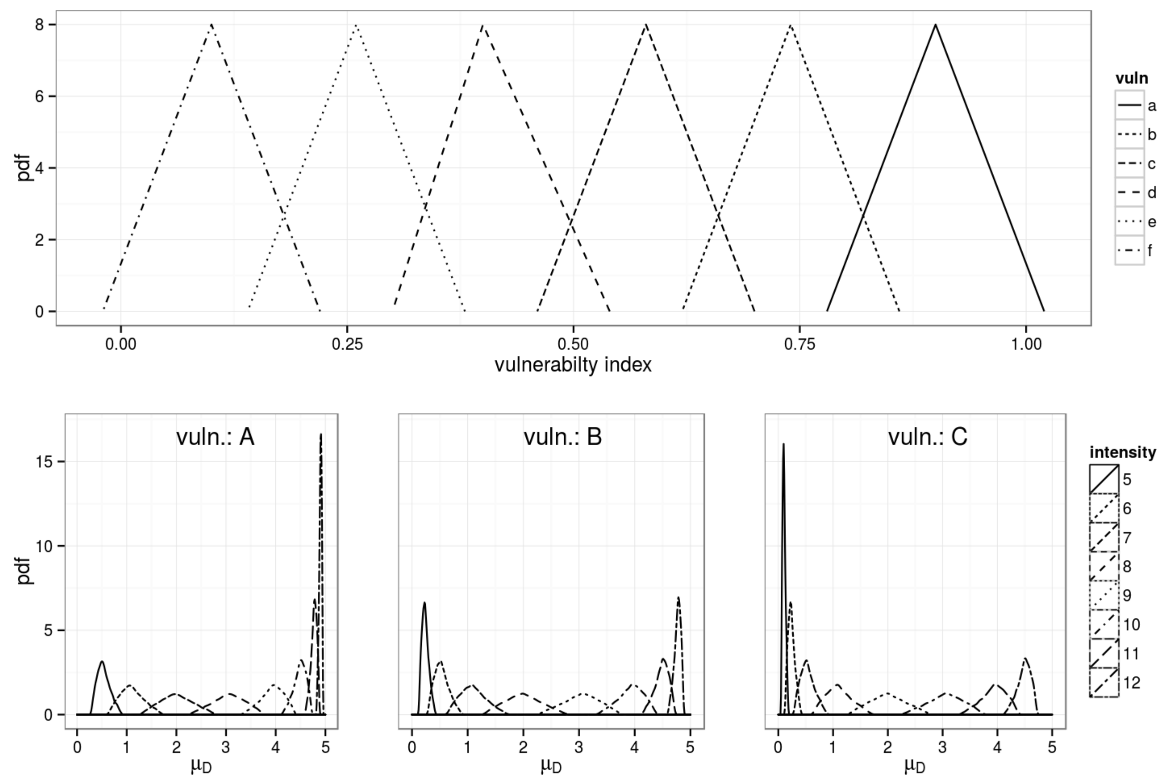

Figure 4. Upper side: probability density function of the vulnerability index for each vulnerability class (A to F). Lower side: corresponding empirical probability density functions for the mean damage grade for increasing values of intensity (from V to XII). Only the distributions for the vulnerability types A, B and C are shown.

Choice of prior distributions

The choice of the prior on the probability distribution of macroseismic intensity is of particular importance, especially in cases where the number of available observations is relatively small. We considered three different approaches (the actual prior distributions are shown in Fig. 5):

- non-informative prior,
- informative prior constrained by the estimated average MI=VIII,
- prior based on expert judgment.

In the first case we suppose that no information whatsoever is available in advance. In this case, by using the principle of indifference (Keynes, 1921), we can assign equal probability to each of the intensity levels. This is also compatible with the principle of maximum entropy, which states that the probability distribution with the largest entropy is the one that best represents the available information (Jaynes, 1957). In the second case, a more objective prior is estimated by noticing that some information about the intensity may be available in advance. For instance, the average value of the shake map estimating the instrumental intensity for the selected area has been used (Faenza et al., 2016) and rounded up to intensity VIII. In order to encode this information into the prior, the principle of maximum entropy is considered. In the third case, a direct assignment of the prior probabilities is carried out following a subjective judgment. In our case, for instance, only the intensities between VI and XI have been considered possible in the considered area, with equal probability in absence of any other significant information. The probability of intensity XII has been set to zero, in consideration of the fact that such an intensity is never used in the practice (Musson et al., 2010; Dowrick et al., 2008). All prior distributions have been normalized such that the probabilities sum up to 1.

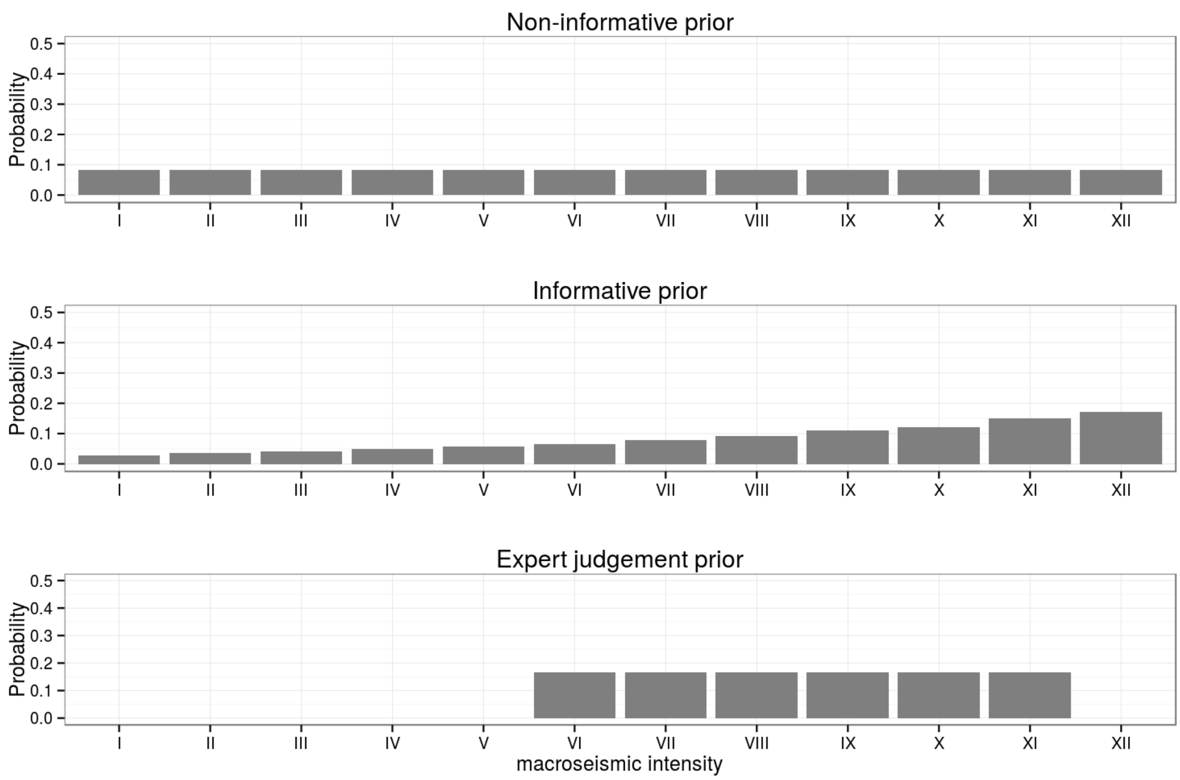

Figure 5. Three different prior distributions on the MI. From the uppermost: constant (non-informative) prior, informative prior conditioned by an estimated average intensity VIII, and a prior based only on expert judgment. In the last case, the probability of intensities $I, \cdots, V$ and XII has been set to zero.

APPLICATION AND RESULTS

For each of the considered localities, the mean damage grade is estimated (according to Eq. 2) from the observed damage scenario, according to the observed vulnerability classes. These intermediate results, listed in Table 3, represent the input to the Bayesian assessment of the intensity.

Table 3. Summary of computed mean damage grades according to the different vulnerability types. The number of observations is also reported, including the total value and the number of observations where at least a damage $D > 0$ was observed. The last three columns list the observed relative frequency of vulnerability types. Only vulnerability types A, B and C have been assigned in the considered region.

Locality	MI INGV	μ_D			No. of observations					Observed freq.		
	(EMS-98)	A	B	C	A	B	C	Total	$D > 0$	A	B	C
Accumuli	VIII	3.5	1.75	1.5	6	15	2	23	19	0.26	0.65	0.09
Amatrice	X	-	2.67	2.25	0	3	4	7	6	0	0.43	0.57
Arquata del Tronto	VIII / IX	2	2.97	0	4	9	1	14	13	0.29	0.64	0.07
Borgo	VIII	2.75	1.74	0.25	4	15	4	23	17	0.17	0.65	0.17
Collalto	VI / VII	4	0.84	0	1	7	4	12	4	0.08	0.58	0.33
Collegentilesco	VI / VII	2.67	0.7	0	6	10	1	17	9	0.35	0.59	0.06
Colli	VI / VII	4	2	-	1	1	0	2	2	0.5	0.5	0
Configno	VI / VII	2.5	2.2	0	2	5	2	9	7	0.22	0.56	0.22
Cornelle di Sotto	VII / VIII	2.26	0.28	0	7	14	5	26	9	0.27	0.54	0.19
Cossito	VIII	4	3.63	1	2	3	1	6	6	0.33	0.5	0.17
Faete	VII	2.66	1.74	0	3	7	2	12	9	0.25	0.58	0.17
Illica	IX	4.4	2.33	-	5	3	0	8	8	0.62	0.38	0
Musicchio	VI / VII	3	1.67	0.66	1	3	3	7	5	0.14	0.43	0.43
Pescara del Tronto	X	4.26	2.6	2.5	8	5	4	17	16	0.47	0.29	0.24
Piedilama	VII	3.2	1.1	1	5	8	4	17	13	0.29	0.47	0.24
Saletta	X	4.5	4	1	4	2	2	8	7	0.5	0.25	0.25
San Cipriano	VII	-	1.34	0.25	0	3	4	7	3	0	0.43	0.57
Santa Lucia	VII	4	0.81	0	2	11	3	16	6	0.12	0.69	0.19
Santi Lorenzo e Flaviano	IX / X	4.16	4	-	6	4	0	10	10	0.6	0.4	0
Scai	VII	-	1.65	0.5	0	9	4	13	8	0	0.69	0.31
Spelonga	VI / VII	0.75	0.61	0.1	4	22	10	36	10	0.11	0.61	0.28
Trisungo	VII	2.29	1.7	0.5	7	10	2	19	14	0.37	0.53	0.11

The procedure described above has been applied (see Eq. 4) to each locality, in order to estimate a posterior probability distribution of the MI from each of the considered priors. From the posterior distribution, two different intensity assignments methods have been implemented: *argmax*, selecting the intensity value with the highest probability, and *weighted*, taking the weighted average of the intensities corresponding to the three highest probabilities. In order to illustrate this approach, Fig. 6 shows the specific case of Arquata del Tronto. In the lower inset the probability density functions (pdf) of the mean damage grade μ_D for the observed vulnerability classes are shown, considering only the three intensity values mostly contributing to the likelihood. We note that intensity VII maximizes the likelihood of observing a μ_D equal to 2 for buildings of vulnerability class A; intensity IX is the most compatible with a μ_D equal to 2.97 for buildings of vulnerability class B. In this case the contrasting information collected during the field survey about the vulnerability classes A and B explains the bimodal posterior distribution. In the case of buildings of vulnerability class C (only one observation in this case) the observation of a μ_D equal to zero narrows down the support of the PDFs, which up to intensity VI almost completely fit within the interval, therefore contributing to increase the likelihood in the lower end of intensity. The final posterior is shown, along with the used (informative) prior, in the upper part of Fig. 6. It can be noted that the relatively high frequency of buildings of vulnerability class B determines the highest peak in the posterior distribution. The continuous vertical line marks the intensity officially assigned by INGV while the dashed lines represent the intensities derived from the posterior distribution following the *argmax* and the *weighted* approaches.

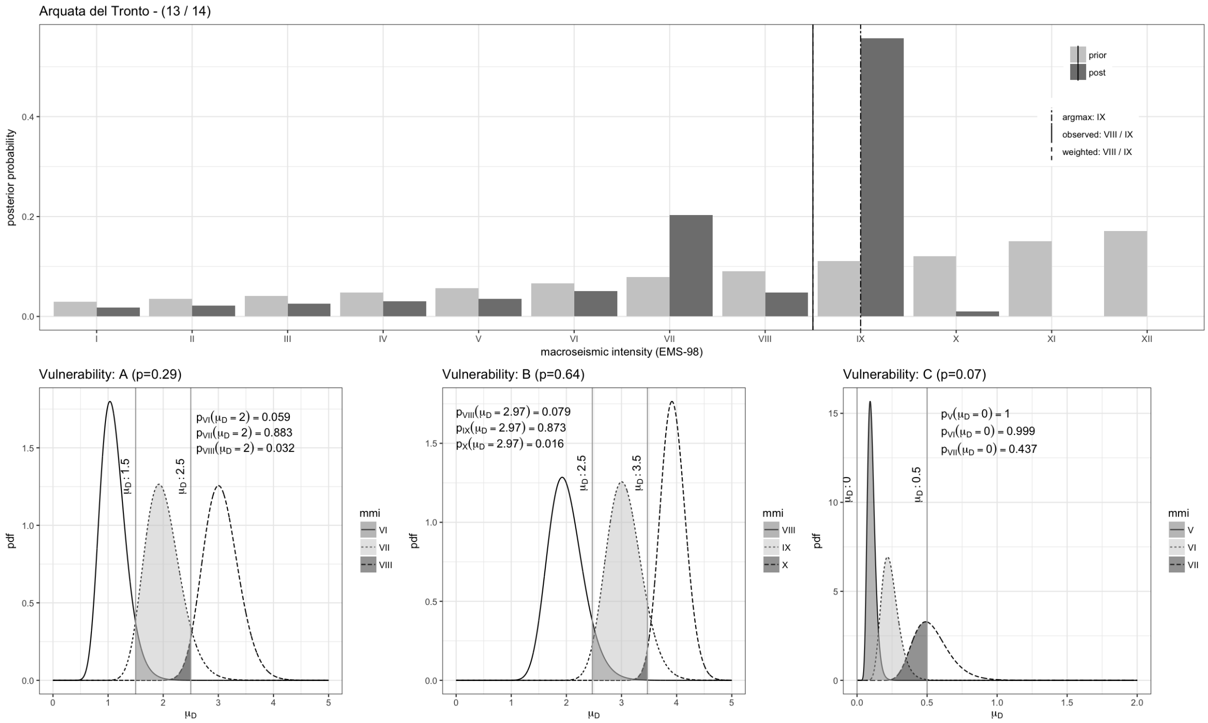

Figure 6. Upper side: comparison of prior and posterior distribution for the settlement of Arquata del Tronto. The continuous vertical line marks the intensity officially assigned by INGV. The dashed lines represent the intensities derived from the posterior distribution by selecting the intensity bin with the highest probability (argmax) or by taking the weighted average of the intensities corresponding to the three highmost bins. Lower side: probability density functions (PDF) of mean damage grade for the observed vulnerability classes. Only the three intensity values contributing significantly to the likelihood are shown.

In Figs. 7 to 9, the posterior distributions and the corresponding intensity assignments are shown for the localities where RRDA damage grading was available for the considered three prior distributions. Intensity values officially assigned by INGV to these settlements (black triangles) are also shown, along with the distribution of the residuals, defined as the difference between the value estimated with the weighted approach and the value officially assigned. The size of the points is proportional to the number of grading used for the estimation. This number is also indicated for each target location, along with the number of gradings with non-zero damage). For both assignment approaches (argmax and weighted), the average residual is also indicated. A comparison of the estimation results according to the different priors and assignment approach is provided in Table 4 in terms of the number of assignments which differ by respectively up to half an intensity degree and up to one intensity degree with respect to the official intensities provided by INGV. As an additional indicator, the last column in the table provides the squared sum of residuals normalized on the number of estimations.

Table 4. Comparison of the estimation results according to the different priors and assignment approaches. The total number of estimations is 22. The last column displays the sum of squared residuals (RSS) normalized on the number of estimations.

prior type	assignment	within half intensity	within one intensity	RSS
flat	weighted	15	19	2.19
flat	argmax	10	16	3.17
informative	weighted	14	18	1.13
informative	argmax	8	16	1.36
expert judgment	weighted	11	17	0.67
expert judgment	argmax	17	20	1.17

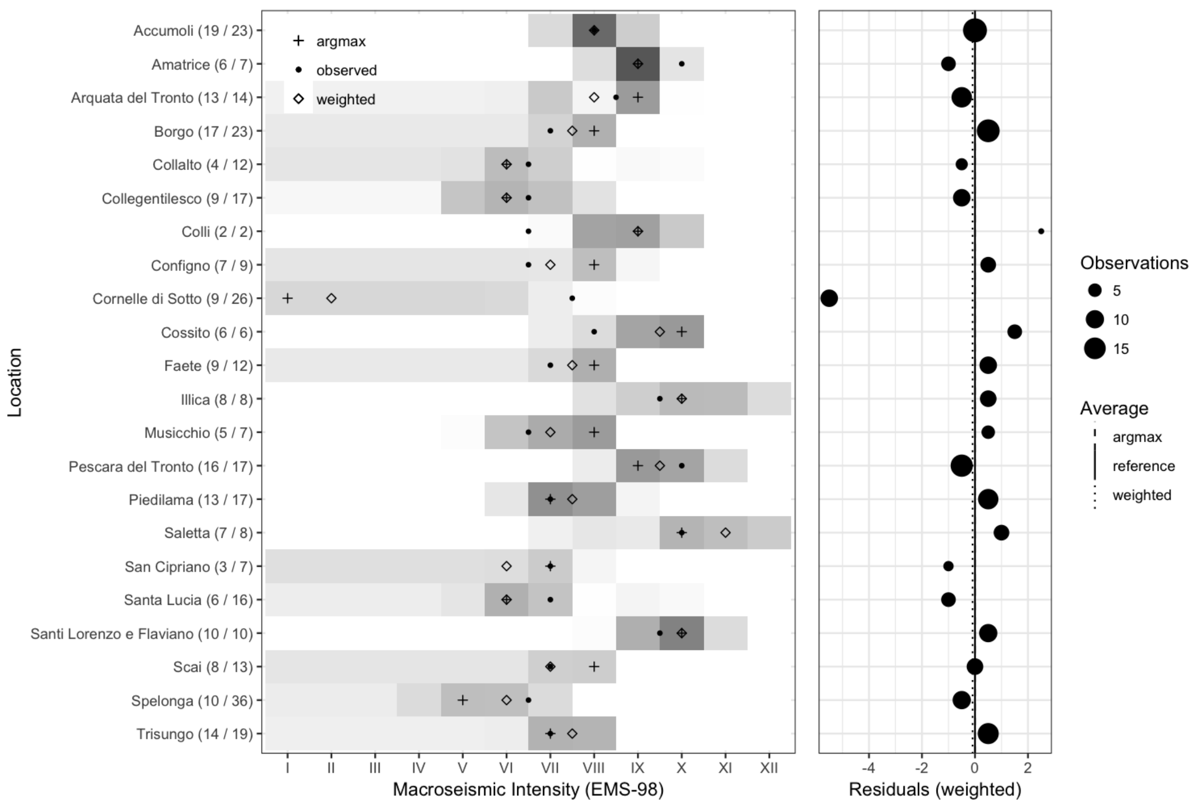

Figure 7. Left: Posterior distribution of MI with uninformative (flat) prior for the considered settlements. In parenthesis are the number of gradings with damage $D > 0$ and the total number). The reference (official INGV) assignment is indicated by a black triangle. Intensity estimated with both the argmax and weighted approaches are also shown. Right: distribution of residuals, defined as the difference between estimated (weighted) and assigned intensity. The size of the points is proportional to the number of available gradings. Vertical lines represent the average residuals, including the zero residual as reference.

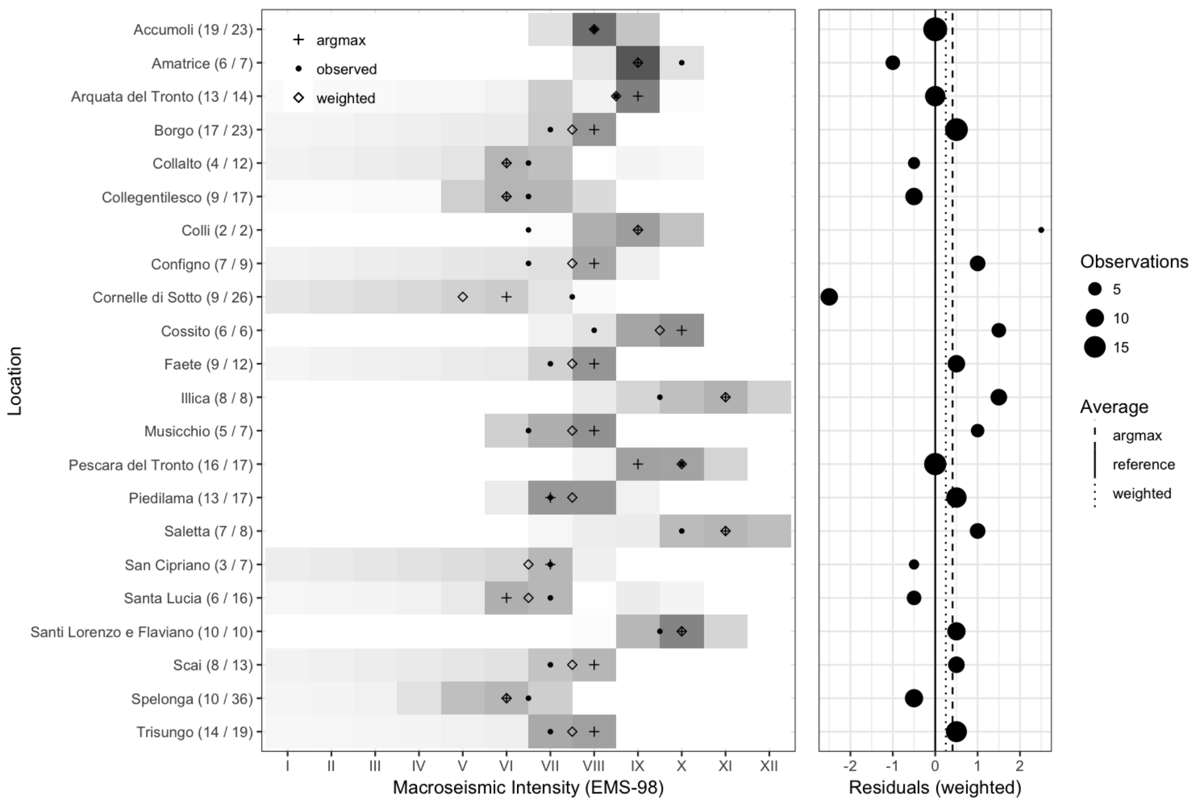

Figure 8. As in Fig. 7 but for posterior distribution of MI with informative prior.

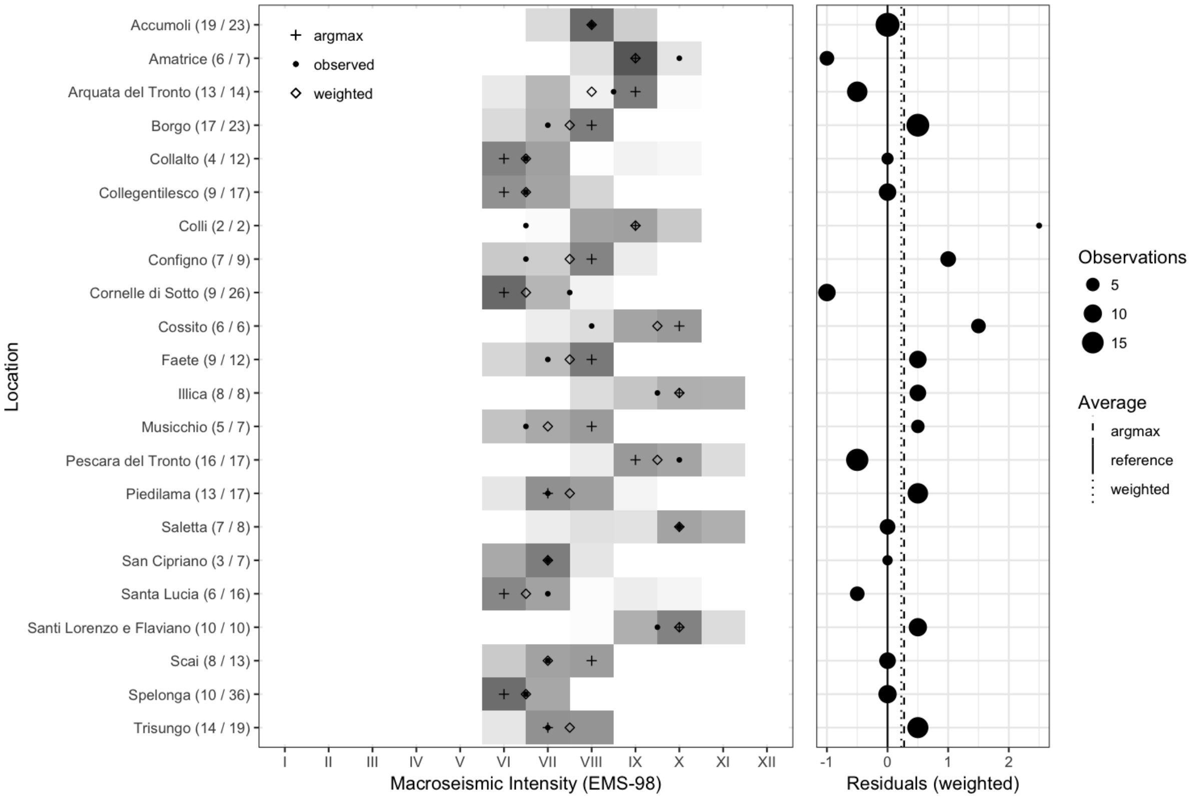

Figure 9. As in Fig. 7 but for posterior distribution of MI with expert judgment-based prior.

DISCUSSION

The results show a good agreement between the intensities estimated following the presented method with respect to the ones officially assigned by INGV through extensive *in situ* investigations. This suggests that a balanced spatial sampling of buildings for inspection may allow for consistent estimates, even with sparse observations. We note that using an uninformative (flat) prior (Fig. 7) the residuals are more widely spread than with the other priors (i.e., the RSS is greater), but the average residuals considering both the *argmax* and the *weighted* assignment methods are close to zero, hence relatively unbiased. In contrast, by using an informative (Fig. 8) or an expert-based (Fig. 9) prior on average a better overall performance is obtained, but with an observable bias. This applies mostly in the cases where the paucity of information leads to highly uncertain distributions, and therefore the prior has a relevant role. Where the observed information is consistent (as happens in most of the cases), the three different priors provide a comparable performance. Among the considered locations, only Cornelle di Sotto and Colli show a significant discrepancy between estimated and assigned intensity. This discrepancy is minimized when a stronger prior is used (Fig. 9). The intensity assignment for Colli is based on only two gradings, hence it should be considered unreliable. Cornelle di Sotto is a very small village located in the municipality of Amatrice, where most of the damage was concentrated in the historical center. The Voronoi cell used to aggregate the individual gradings to this settlement also partly included neighboring villages, where less damage was observed. Although the use of Voronoi tessellation allows for a straightforward mapping of the grading to the settlements based solely on their centroidal coordinates, if a high spatial variability in MI is observed (due, for example, to local site amplification effects), a further bias may be introduced. Remarkably, although the car with the mobile mapping system was often not allowed to enter the so called red areas, where most of the collapses occurred, there is no observable negative bias in the intensity assignments. On the contrary, a small positive bias (less than half intensity grade) can be observed on average when using informative and expert-judgment priors. In the case of the informative prior, this positive bias may be imputed to the monotonically increasing shape of the distribution, due to the application of the principle of maximum entropy. In fact the arithmetic mean of the official INGV intensities is 7.73, very close to the average value VIII estimated from the instrumental shake map (Faenza et al., 2016) and used to constrain the prior distribution. The use of a strong prior such as the expert-judgment one, further increases the performance of the procedure. In most cases intensity values greater than XI can be safely ruled out by setting to zero the corresponding prior probability, however this type of prior should be employed with care, since an irreversible constrain is created which cannot be further modified by incoming information. Finally, two methodologies have been considered to assign a single intensity from the probability distribution. According to the obtained results, the assignment based on the weighted combination of the three most likely intensity values (indicated as *weighted*) shows a consistently better performance with respect to using the intensity value with highest likelihood (*argmax*).

CONCLUSIONS AND OUTLOOK

An innovative methodology is proposed to provide a rapid estimation of macroseismic intensity, in terms of the EMS-98 scale, based on the observed damage to the built environment. Despite being based on a small number of gradings, the estimated intensities are in good agreement with the ones officially assigned by INGV through extensive in situ investigations. A consistent probabilistic estimation of the macroseismic intensity in different geographical locations can therefore be carried out, integrating the collected information with ancillary data and expert judgment through the use of a Bayesian updating framework. The following concluding remarks can be done:

- The web-based reconnaissance platform (RRDA), based on visual data collected through mobile mapping, allows for the involvement of a potentially high number of skilled surveyors, working remotely. The RRDA platform could in fact be easily scaled up, allowing the prompt collection of more statistically significant datasets, and contributing to improving the situational awareness of civil protection authorities and decision makers.

- The overall procedure has been designed to minimize the amount of subjective judgment and provide a transparent, traceable processing scheme. The immediate availability of the collected data (including both the individual evaluation of the experts and the related georeferenced panoramic images) can contribute to the prompt recalibration of fragility and vulnerability models. The proposed procedure would also benefit from the integration of reconnaissance data provided by independent surveying missions.

- Since only intensities greater than V are associated with physical damage to structures, lower intensity grades cannot be reliably estimated with this methodology. The integration of complementary data such as, for instance, crowd-sourced reports on felt earthquakes, could contribute filling in information on the lower intensity grades.

- While the damage grades are well described by the EMS-98 formulation, the assignment of vulnerability classes is more uncertain and relies heavily on the experience of the surveyor. However, since the RRDA user interface was originally designed to collect structural and non-structural features according to a standard taxonomy (GEM v2.0), in future applications, the vulnerability class (and hence the vulnerability index) might be assigned in an unsupervised way based on clearly observable properties, minimizing the amount of subjective judgment.

- The use of the data provided by the Copernicus Emergency Mapping Service exemplifies the integration of qualified information into the process from a very early stage and over a broad area, showing how the damage grading from satellite imagery may actively complement the data collected via a mobile mapping system with information on the most damaged areas, which are likely not accessible to a direct survey.

ACKNOWLEDGMENT

This study has been supported by the GFZ Hazard and Risk Team (HART) program. We are grateful to the Italian Department for Civil Protection for their support during our field operations, and would also like to acknowledge the kind assistance of the National Firefighters Corps and the Italian Army in the epicentral area. We are grateful to the two unknown reviewers, and to Kishor Jaiswal (USGS) whose constructive comments and suggestions further improved the manuscript. We also thank Kevin Fleming for the careful proofreading.

REFERENCES

Anzidei, M. and Pondrelli, S., 2016. The Amatrice seismic sequence: preliminary data and results. *Annals of Geophysics* **59**.

Azzaro, R., Tertulliani, A., Bernardini, F., Camassi, R., Del Mese, S., Ercolani, E., Graziani, L., Locati, M., Maramai, A., Pessina, V., Rossi, A., Rovida, A., Albini, P., Arcoraci, L., Berardi, M., Bignami, C., Brizuela, B., Castellano, C., Castelli, V., D'Amico, S., D'Amico, V., Fodarella, A., Leschiutta, I., Piscini, A., and Sbarra, M., 2016. The 24 august 2016 amatrice earthquake: Macroseismic survey in the damage area and EMS intensity assessment. *Annals of Geophysics* **59**. doi:10.4401/ag-7203.

Boccardo, P. and Tonolo, F. G., 2015. Remote sensing role in emergency mapping for disaster response. In *Engineering Geology for Society and Territory - Volume 5: Urban Geology, Sustainable Planning and Landscape Exploitation*, pp. 17–24. ISBN 9783319090481. doi:10.1007/978-3-319-09048-13.

Bormann, P. (ed.), 2011. *New Manual of Seismological Observatory Practice (NMSOP-2)*. GFZ German Research Centre for Geosciences, Potsdam: IASPEI.

Copernicus, 2016. Emergency Management Service (© 2016 European Union), activation SRM177.

Dowrick, D. J., Hancox, G. T., Perrin, N. D., and Dellow, G. D., 2008. The Modified Mercalli intensity scalerevisions arising from New Zealand experience. *Bulletin of the New Zealand Society for Earthquake Engineering* **41**, 193–205.

Faenza, L., Lauciani, V., and Michelini, A., 2016. The shakemaps of the Amatrice, M6, earthquake. *Annals of Geophysics* **59**, 1–8. doi:10.4401/ag-7238.

Freire, S., Florczyk, A., Ehrlich, D., and Pesaresi, M., 2015. Remote sensing derived continental high resolution built-up and population geoinformation for crisis management. In *International Geoscience and Remote Sensing Symposium (IGARSS)*, vol. 2015-November, pp. 2677–2679. ISBN 9781479979295. doi:10.1109/IGARSS.2015.7326364.

Galli, P., Peronace, E., Bramerini, F., Castenetto, S., Naso, G., Cassone, F., and Pallone, F., 2016. The MCS intensity distribution of the devastating 24 august 2016 earthquake in central Italy (Mw6.2). *Annals of Geophysics* **59**. doi:10.4401/ag-7287.

Gelman, A., Carlin, J. B., Stern, H. S., and Rubin, D. B., 2004. *Bayesian Data Analysis*. ISBN 978-1-4398-9820-8, 696 pp. doi:10.1007/s13398-014-0173-7.2.

Giovinazzi, S. and Lagomarsino, S., 2002. A Method for the Vulnerability Analysis of Built-up areas. In *Proc. of International Conference on Earthquake Loss Estimation and Risk Reduction*, pp. 1–16.

Giovinazzi, S. and Lagomarsino, S., 2004. A Macroseismic Method for the Vulnerability Assessment of Buildings. *13th World Conference on Earthquake Engineering* pp. 1–6.

Grünthal, G., 1998. *European Macroseismic Scale 1998*, vol. 15. ISBN 2879770084, 100 pp.

Jaynes, E. T., 1957. Information theory and statistical mechanics. *Physical Review* **106**, 620–630. doi:10.1103/PhysRev.106.620.

Keynes, J. M., 1921. *A Treatise on Probability*. Macmillan and Company, Ltd., 41–64 pp.

Lagomarsino, S. and Giovinazzi, S., 2006. Macroseismic and mechanical models for the vulnerability and damage assessment of current buildings. *Bulletin of Earthquake Engineering* **4**, 415–443. doi: 10.1007/s10518-006-9024-z.

Medvedev, S. V., Sponheuer, W., and Karnik, V., 1965. *Seismic intensity scale version MSK 1964*. *Tech. rep.*, Academy of Sciences of the USSR, Soviet Geophysical Committee, Moscow.

Musson, R. M., Grünthal, G., and Stucchi, M., 2010. The comparison of macroseismic intensity scales. *Journal of Seismology* **14**, 413–428. doi:10.1007/s10950-009-9172-0.

Musson, R. M. W., 2012. Intensity and Intensity Scales. *New manual of seismological observatory practice 2* pp. 1–41. doi:10.2312/GFZ.NMSOP-2.

Pittore, M. and Wieland, M., 2013. Toward a rapid probabilistic seismic vulnerability assessment using satellite and ground-based remote sensing. *Natural Hazards* **68**, 115–145. doi:10.1007/s11069-012-0475-z.

Pittore, M., Wieland, M., Errize, M., Kariptas, C., and Güngör, I., 2015. Improving Post-Earthquake Insurance Claim Management: A Novel Approach to Prioritize Geospatial Data Collection. *ISPRS International Journal of Geo-Information* **4**, 2401–2427. doi:10.3390/ijgi4042401.

Richter, C. F., 1958. *Elementary Seismology*.

Sieberg, A., 1931. Geologie der Erdbeben. In Gutenberg, B. (ed.), *Handbuch der Geophysik*, pp. 552–554. Borntraeger, Gebrüder, Berlin.

Stover, C. W. and Coffman, J. L., 1993. *Seismicity of the United States, 1568-1989 (Revised)*. United States Government Printing Office (Washington).

Watson, D., 1993. Spatial tessellations: concepts and applications of voronoi diagrams. *Computers & Geosciences* **19**, 1209–1210. doi:10.1016/0098-3004(93)90024-Y.

Wood, H. O. and Neumann, F., 1931. Modified Mercalli Intensity Scale of 1931. *Bulletin of the Seismological Society of America* **21**, 277–283.

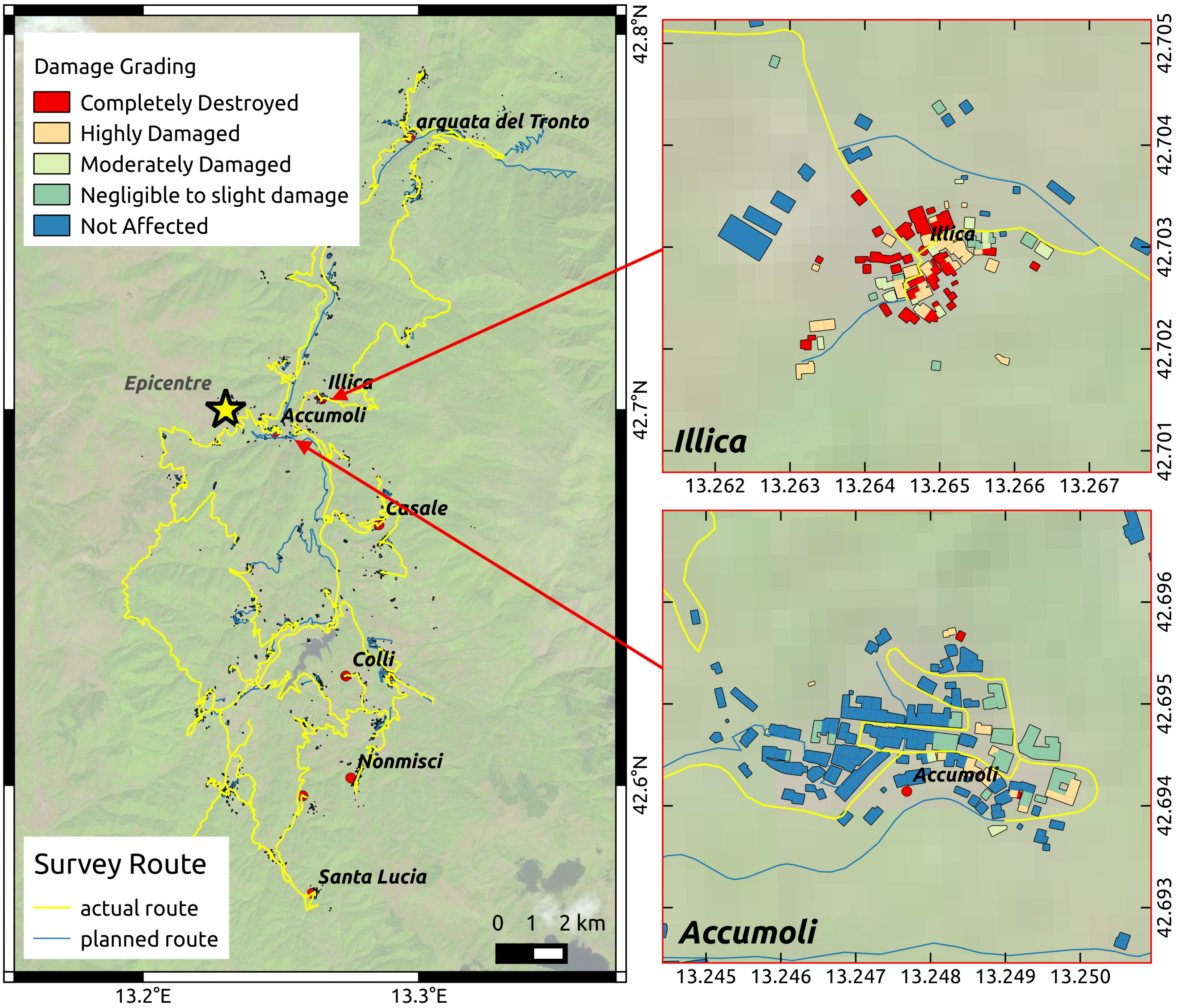

Damage Grading
Completely Destroyed
Highly Damaged
Moderately Damaged
Negligible to slight damage
Not Affected
arquata del Tronto
Epicentre
Illica
Accumoli
Casale
Colli
Nonmisci
Santa Lucia
Survey Route
actual route
planned route
0 1 2 km
42.8°N
42.7°N
42.6°N
13.2°E
13.3°E
13.262
13.263
13.264
13.265
13.266
13.267
42.705
42.704
42.703
42.702
42.701
13.245
13.246
13.247
13.248
13.249
13.250
42.696
42.695
42.694
42.693

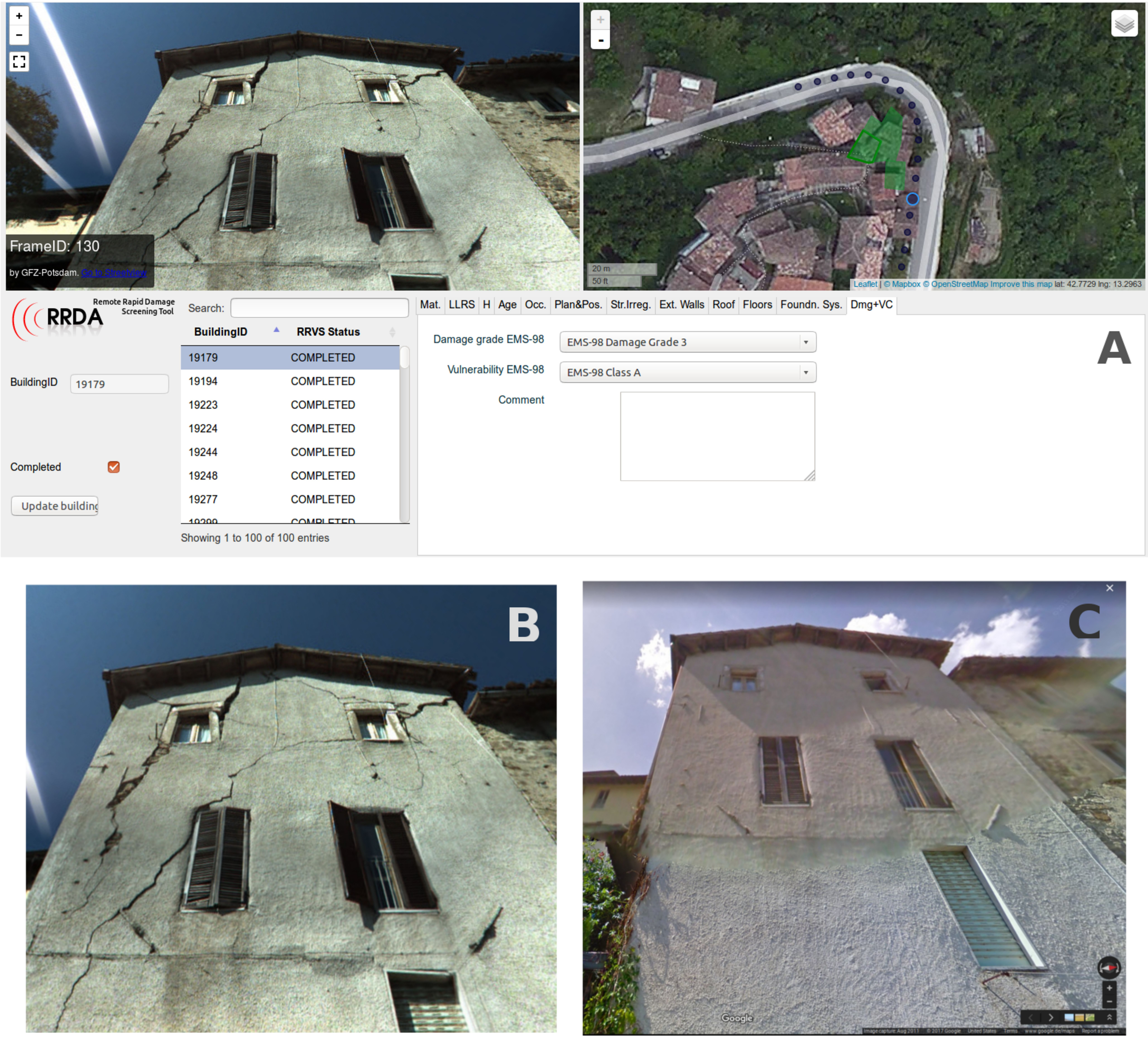

FrameID: 130
by GFZ-Potsdam. Go to Streetview
20 m
50 ft
Leaflet | © Mapbox © OpenStreetMap Improve this map lat: 42.7729 lng: 13.2963
Remote Rapid Damage Screening Tool
RRDA
Search:
BuildingID
RRVS Status
19179 COMPLETED
19194 COMPLETED
19223 COMPLETED
19224 COMPLETED
19244 COMPLETED
19248 COMPLETED
19277 COMPLETED
Showing 1 to 100 of 100 entries
BuildingID
19179
Completed
Update building
Mat. LLRS H Age Occ. Plan&Pos. Str.Irreg. Ext. Walls Roof Floors Foundn. Sys. Dmg+VC
Damage grade EMS-98
EMS-98 Damage Grade 3
Vulnerability EMS-98
EMS-98 Class A
Comment
A
B
C
Google

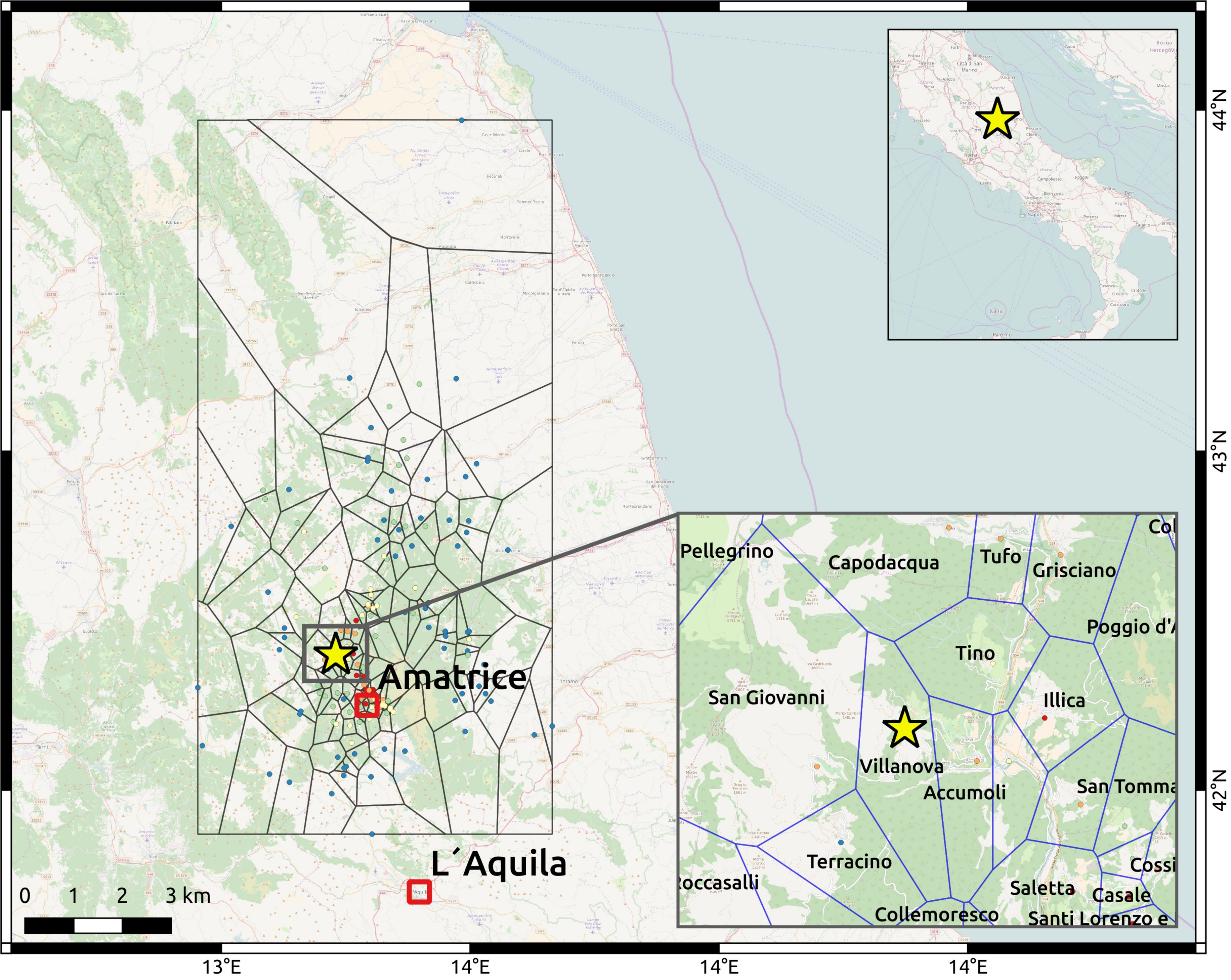

Amatrice
L´Aquila
0
1
2
3 km
Pellegrino
Capodacqua
Tufo
Grisciano
Poggio d'A
Tino
San Giovanni
Illica
Villanova
Accumoli
San Tomma
Terracino
Roccasalli
Saletta
Casale
Cossi
Collemoresco
Santi Lorenzo e
Col
44°N
43°N
42°N
13°E
14°E
14°E
14°E

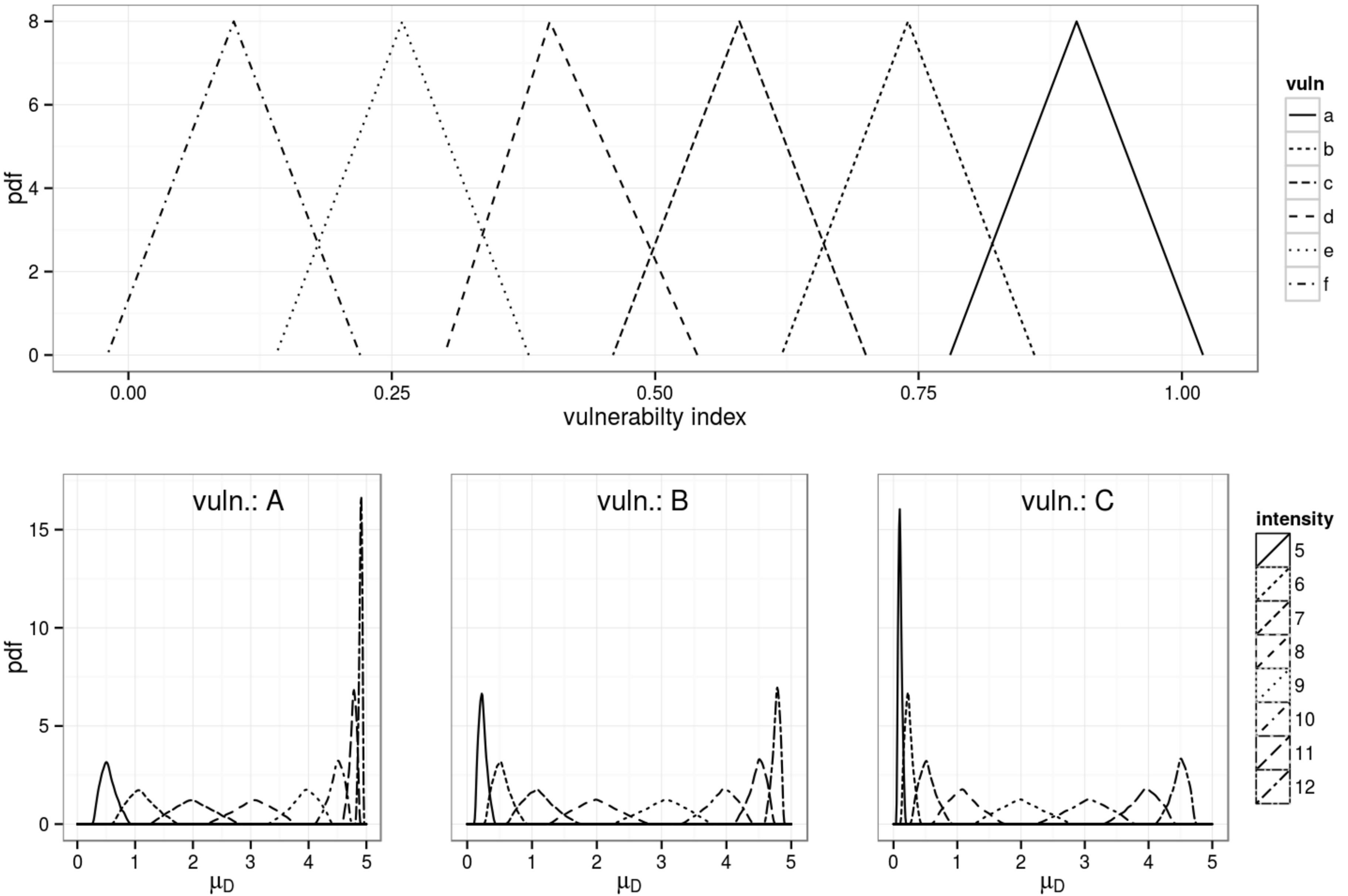

pdf
vulnerabilty index
0.00
0.25
0.50
0.75
1.00
0
2
4
6
8
vuln
a
b
c
d
e
f
vuln.: A
vuln.: B
vuln.: C
0
5
10
15
0
1
2
3
4
5
μ_D
intensity
5
6
7
8
9
10
11
12

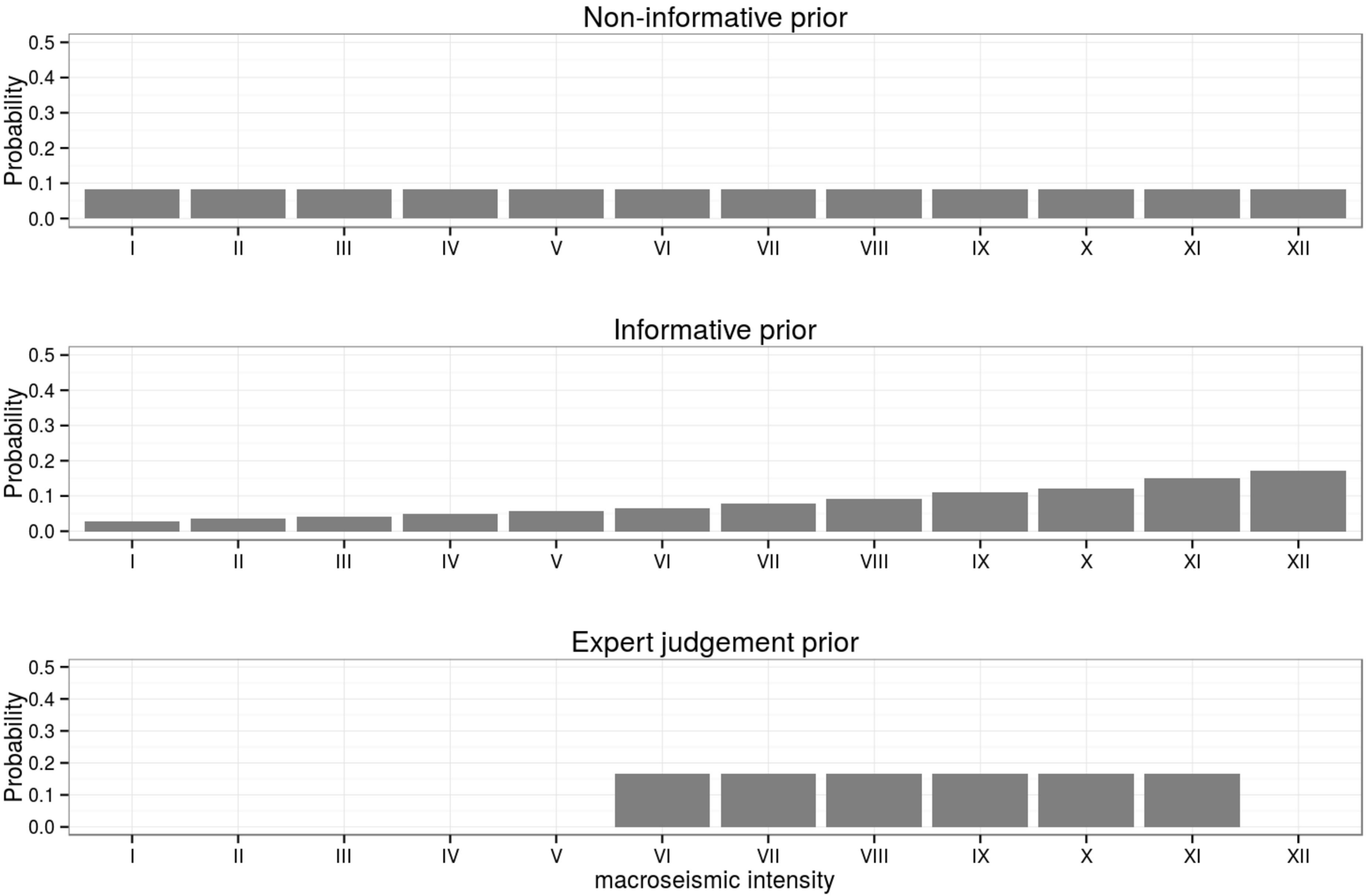

Non-informative prior
Informative prior
Expert judgement prior
Probability
0.0
0.1
0.2
0.3
0.4
0.5
I
II
III
IV
V
VI
VII
VIII
IX
X
XI
XII
macroseismic intensity

Arquata del Tronto - (13 / 14)
posterior probability
macroseismic intensity (EMS-98)
prior
post
argmax: IX
observed: VIII / IX
weighted: VIII / IX
Vulnerability: A (p=0.29)
$p_{VI}(\mu_D = 2) = 0.059$
$p_{VII}(\mu_D = 2) = 0.883$
$p_{VIII}(\mu_D = 2) = 0.032$
μ_D : 1.5
μ_D : 2.5
Vulnerability: B (p=0.64)
$p_{VIII}(\mu_D = 2.97) = 0.079$
$p_{IX}(\mu_D = 2.97) = 0.873$
$p_{X}(\mu_D = 2.97) = 0.016$
μ_D : 2.5
μ_D : 3.5
Vulnerability: C (p=0.07)
$p_{V}(\mu_D = 0) = 1$
$p_{VI}(\mu_D = 0) = 0.999$
$p_{VII}(\mu_D = 0) = 0.437$
μ_D : 0
μ_D : 0.5
pdf
μ_D
mmi

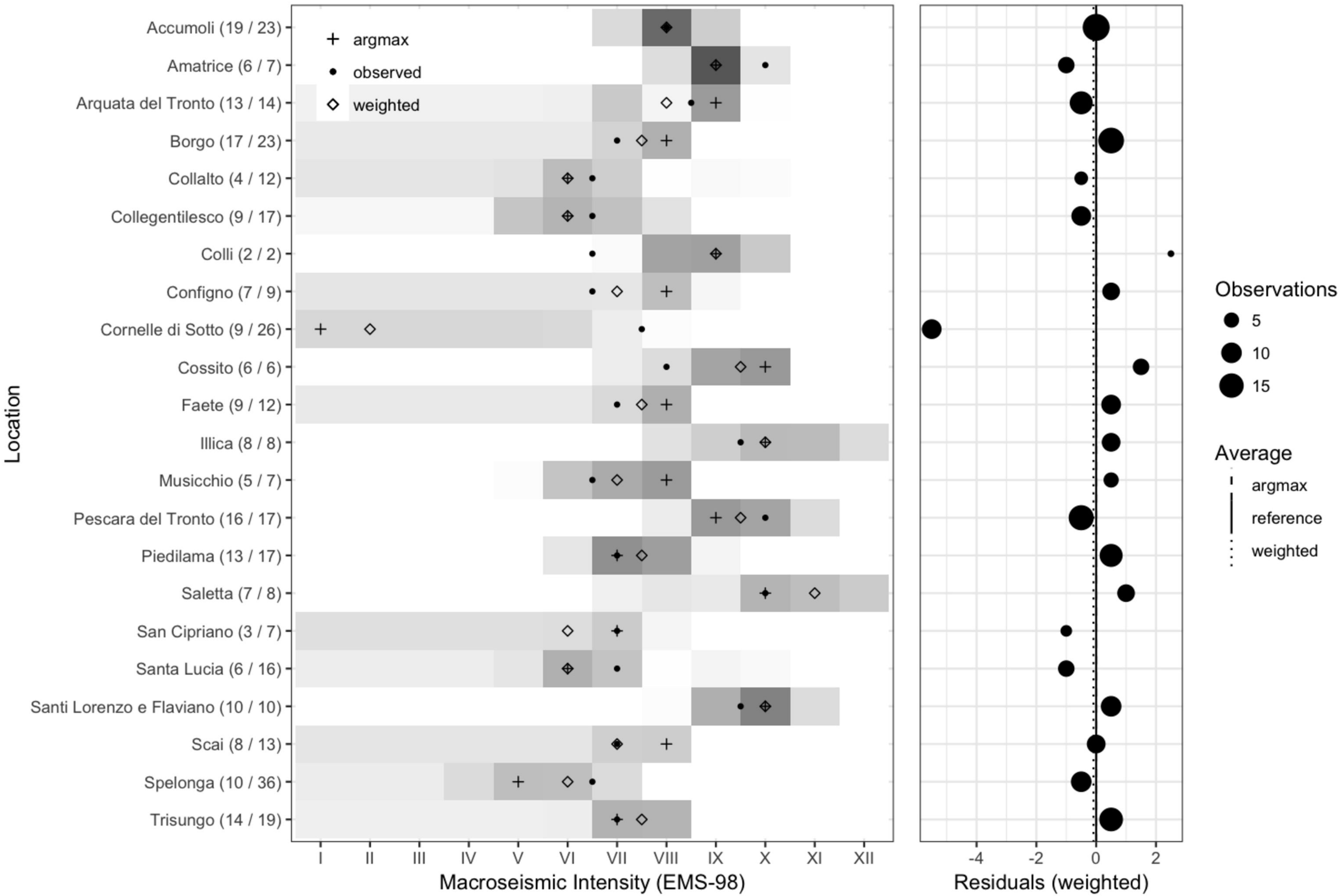

argmax
observed
weighted
Accumoli (19 / 23)
Amatrice (6 / 7)
Arquata del Tronto (13 / 14)
Borgo (17 / 23)
Collalto (4 / 12)
Collegentilesco (9 / 17)
Colli (2 / 2)
Configno (7 / 9)
Cornelle di Sotto (9 / 26)
Cossito (6 / 6)
Faete (9 / 12)
Illica (8 / 8)
Musicchio (5 / 7)
Pescara del Tronto (16 / 17)
Piedilama (13 / 17)
Saletta (7 / 8)
San Cipriano (3 / 7)
Santa Lucia (6 / 16)
Santi Lorenzo e Flaviano (10 / 10)
Scai (8 / 13)
Spelonga (10 / 36)
Trisungo (14 / 19)
Location
I
II
III
IV
V
VI
VII
VIII
IX
X
XI
XII
Macroseismic Intensity (EMS-98)
-4
-2
0
2
Residuals (weighted)
Observations
5
10
15
Average
argmax
reference
weighted

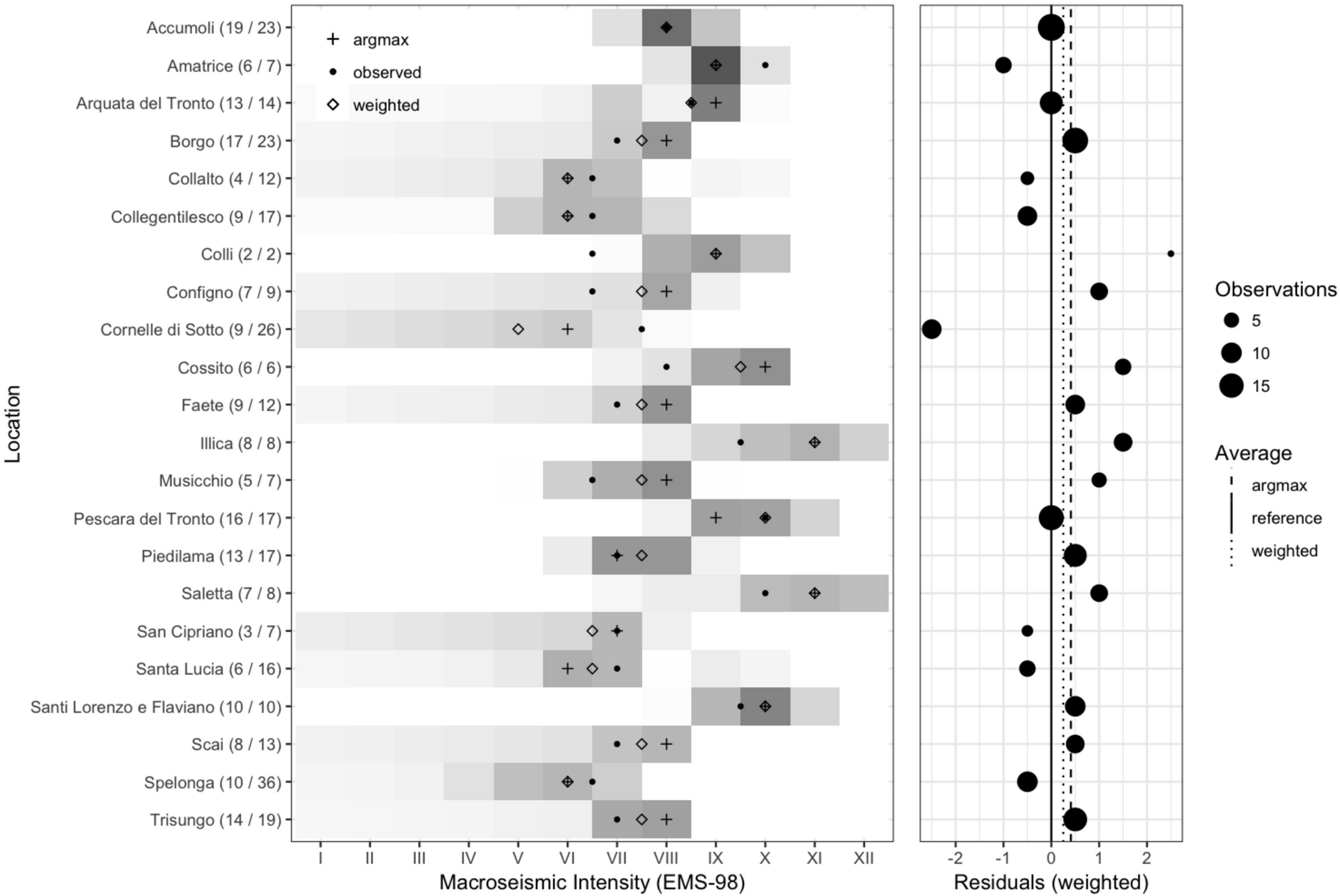
Accumoli (19 / 23)
Amatrice (6 / 7)
Arquata del Tronto (13 / 14)
Borgo (17 / 23)
Collalto (4 / 12)
Collegentilesco (9 / 17)
Colli (2 / 2)
Configno (7 / 9)
Cornelle di Sotto (9 / 26)
Cossito (6 / 6)
Faete (9 / 12)
Illica (8 / 8)
Musicchio (5 / 7)
Pescara del Tronto (16 / 17)
Piedilama (13 / 17)
Saletta (7 / 8)
San Cipriano (3 / 7)
Santa Lucia (6 / 16)
Santi Lorenzo e Flaviano (10 / 10)
Scai (8 / 13)
Spelonga (10 / 36)
Trisungo (14 / 19)
Location
argmax
observed
weighted
I
II
III
IV
V
VI
VII
VIII
IX
X
XI
XII
Macroseismic Intensity (EMS-98)
-2
-1
0
1
2
Residuals (weighted)
Observations
5
10
15
Average
argmax
reference
weighted

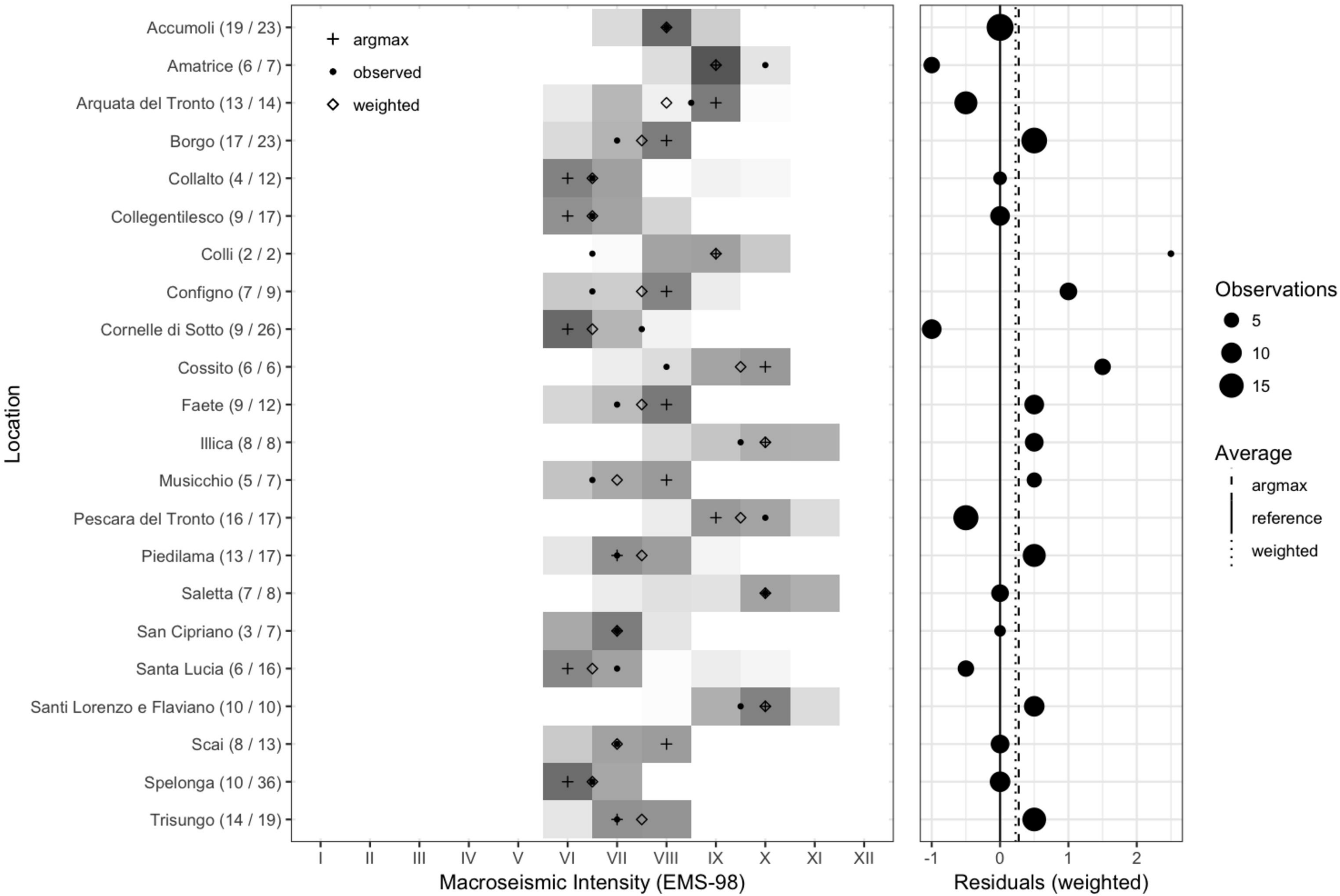

argmax
observed
weighted
Accumoli (19 / 23)
Amatrice (6 / 7)
Arquata del Tronto (13 / 14)
Borgo (17 / 23)
Collalto (4 / 12)
Collegentilesco (9 / 17)
Colli (2 / 2)
Configno (7 / 9)
Cornelle di Sotto (9 / 26)
Cossito (6 / 6)
Faete (9 / 12)
Illica (8 / 8)
Musicchio (5 / 7)
Pescara del Tronto (16 / 17)
Piedilama (13 / 17)
Saletta (7 / 8)
San Cipriano (3 / 7)
Santa Lucia (6 / 16)
Santi Lorenzo e Flaviano (10 / 10)
Scai (8 / 13)
Spelonga (10 / 36)
Trisungo (14 / 19)
Location
I II III IV V VI VII VIII IX X XI XII
Macroseismic Intensity (EMS-98)
-1 0 1 2
Residuals (weighted)
Observations
5
10
15
Average
argmax
reference
weighted